NASA TECHNICAL NOTE

NASA TN D-2314

NASA TN D-2314

FLIGHT VIBRATION DATA OF THE AEROBEE 150A SOUNDING ROCKET

by James A. Nagy and Gomer L. Coble, Jr.

Goddard Space Flight Center
Greenbelt, Md.

NATIONAL AERONAUTICS AND SPACE ADMINISTRATION • WASHINGTON, D. C. • JUNE 1964

FLIGHT VIBRATION DATA OF THE AEROBEE 150A SOUNDING ROCKET

By James A. Nagy and Gomer L. Coble, Jr.

Goddard Space Flight Center
Greenbelt, Maryland

NATIONAL AERONAUTICS AND SPACE ADMINISTRATION

For sale by the Office of Technical Services, Department of Commerce,
Washington, D.C. 20230 -- Price $0.75

FLIGHT VIBRATION DATA OF THE AEROBEE 150A SOUNDING ROCKET

by

James A. Nagy and Gomer L. Coble, Jr.

Goddard Space Flight Center

SUMMARY

Two channels of vibration data were obtained from each of two Aerobees launched from Wallops Island. Vibration data for two vehicle axes were obtained during the powered phase of flight from accelerometers mounted on the attitude control system (ACS). The highest vibration levels occurred while the rocket was rail guided. During this period the average levels were approximately 7 g's RMS longitudinally and 7-8 g's RMS laterally. After tower exit vibration levels dropped to low values and built up slightly at maximum q and at rocket motor burnout. Previous flights of three-fin Aerobees indicated vibration levels, during the tower portion of flight, which were three times greater than those of the four-fin Aerobees.

CONTENTS

Summary i

INTRODUCTION 1

THE FOUR-RAIL TOWER 1

FLIGHT TIME HISTORY 5

INSTRUMENTATION 5

NASA 4.20 Aerobee Rocket 5
NASA 4.68 Aerobee Rocket 7

DATA REDUCTION 7

TEST RESULTS 8

NASA 4.20 Aerobee Rocket 8
NASA 4.68 Aerobee Rocket 13

CONCLUSIONS AND RECOMMENDATIONS 18

Bibliography 26

FLIGHT VIBRATION DATA OF THE AEROBEE 150A SOUNDING ROCKET

by
James A. Nagy and Gomer L. Coble, Jr.
Goddard Space Flight Center

INTRODUCTION

The primary objective of two Aerobee 150A rocket flights (NASA 4.20 launched on June 26, 1961 and NASA 4.68 launched on January 13, 1962) was to flight test the maneuvering capability, holding, and acquisition accuracy of a three axis, gyro referenced and controlled, rocket attitude control system. As a secondary effort, both rockets carried two scientific experiments and a vibration experiment. The objective of the latter is to provide launch and flight vibration data. Rocket borne payloads are required to demonstrate their ability to withstand the exposure to vibration encountered during flight. Laboratory vibration tests are conducted to provide an added safeguard against vibration damage.

The vibration environment must be adequately defined if laboratory test criteria are to be meaningful. Thus, the value of the test program is largely a function of the available flight data. In the case of Aerobee, some data were available from a Fort Churchill launch of a three-fin Aerobee*. These data indicated high levels and were questioned as not being applicable to four-fin Aerobees launched from Wallops Island.

The purpose of this report is to present the data measured during two flights of the four-fin Aerobees. The vehicle and launch tower configurations are described and time histories of flight performance are presented.

THE FOUR-RAIL TOWER

The Wallops Island Aerobee four-rail tower (Figure 1) is 160 feet high and is supported on a gimbal-mounting 80 feet from the base. The tower is enclosed for all-weather operation. Figure 2 shows the pre-launch vehicle-tower arrangement. Tower azimuth and tilt are controlled from the blockhouse so that rockets can be fired in a direction to compensate for wind effects on the vehicle, thus minimizing dispersion of the impact point. Two blast doors at the bottom of the building are opened to relieve smoke and blast pressure (Figure 1). Figure 3 shows the four-rail tower with the rail designations referred to throughout this report.

*Roth, C. E., Jr., and Swanson, R. S., "Environmental Measurements in Sounding Rockets," IES Proceedings, 1961.

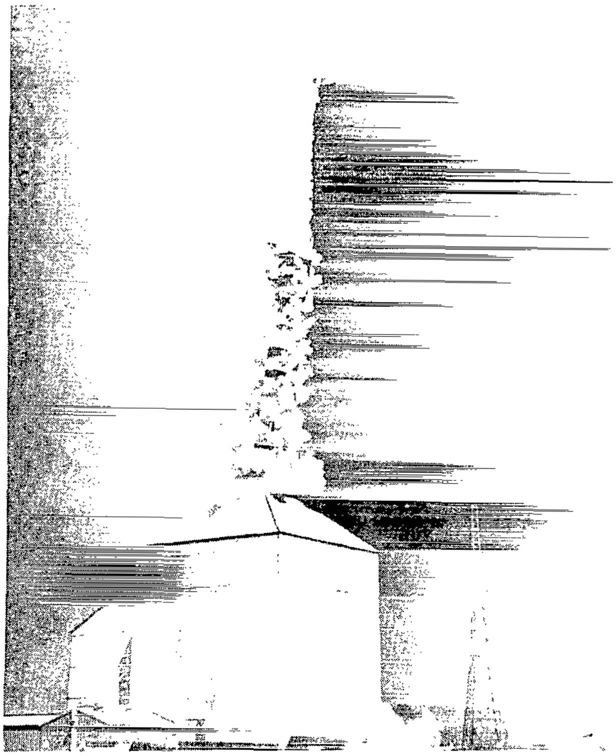

Figure 1—Aerobee Launch Facility
Wallops Island, Virginia.

Figure 2—Aerobee Launch Facility, interior view.

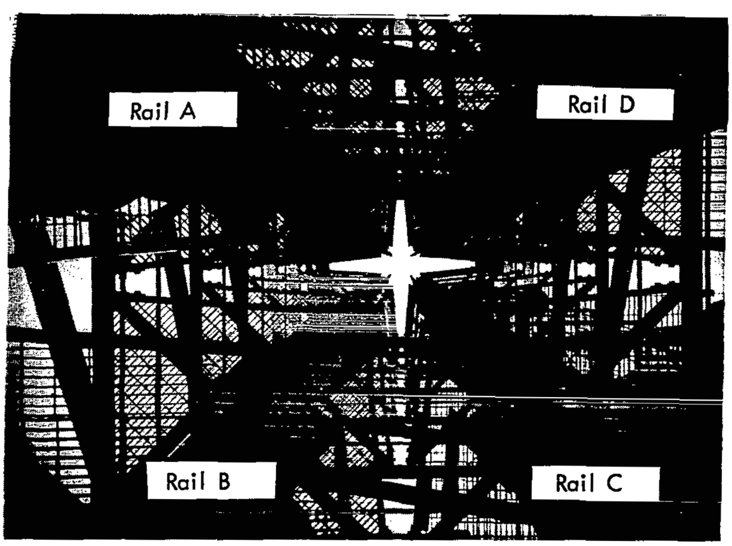

Figure 3—Aerobee Launch Tower, looking up.

The Aerobee 150A sounding rocket is an expendable, boosted, fin-stabilized, free-flight liquid-propellant rocket-powered vehicle. It has an extended cylindrical configuration with a 31-caliber, ogival nose (Figure 4). Payloads are mounted inside the nose structure and, if desired, a payload extension and a camera extension are utilized. Four fixed-fins are spaced 90 degrees apart around the aft end of the rocket to provide aerodynamic stability. Figure 5 presents the general arrangement of the Aerobee 150A. These fins are adjustable and may be canted from 0°0' to 0°20' for a desired roll-rate. The rocket is boosted from a four-rail tower by a solid-propellant booster. Initial guidance is provided by riding lugs on the rocket (fore and aft), booster riding lugs, and a booster guide lug (Figures 6 and 7). Replicas of the fore and aft rocket riding lugs of NASA 4.48, which were recovered after the operation, are shown in Figures 8 and 9, respectively. The booster is a high-thrust, short duration rocket motor. The booster fins are installed at a preset angle of 2°30' to impart initially a high-roll rate to the vehicle as it leaves the launching tower. The booster and vehicle are position-mated by a thrust structure and remain together by gravity and/or the overriding booster thrust until booster burnout.

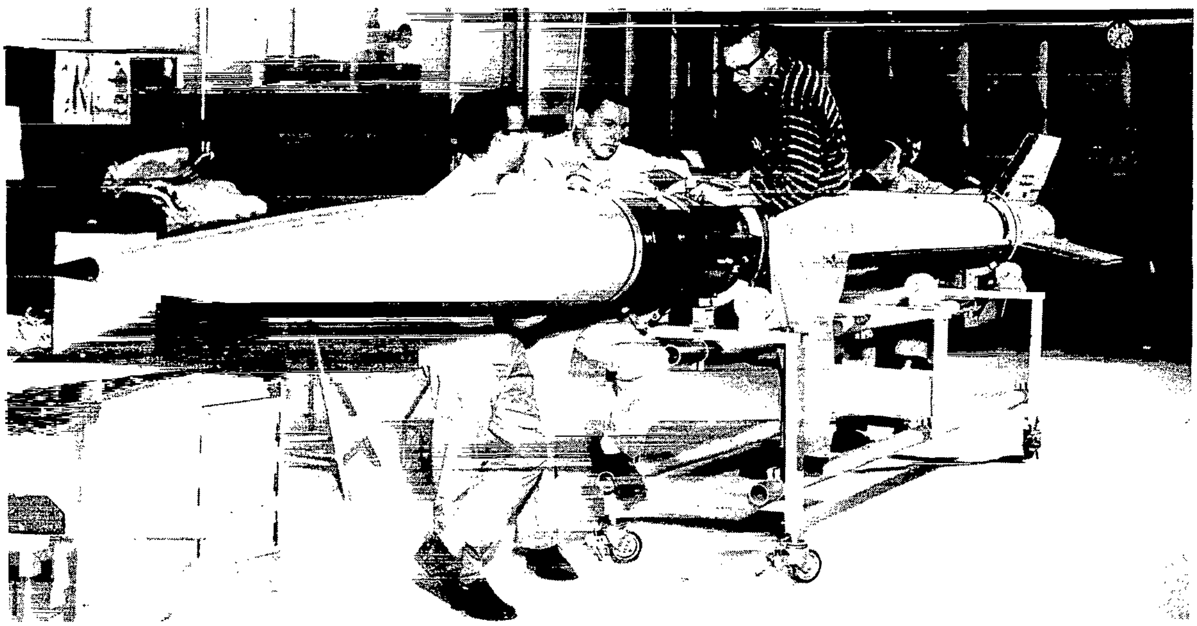

Figure 4—Aerobee 150A.

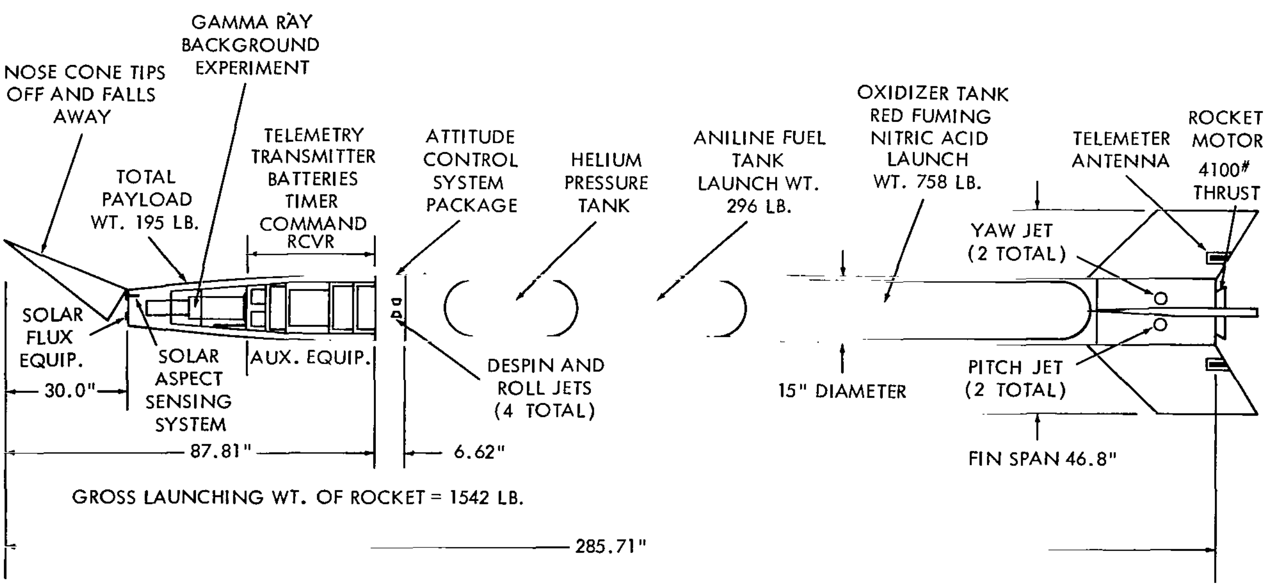

Figure 5—Aerobee-150A, general arrangement.

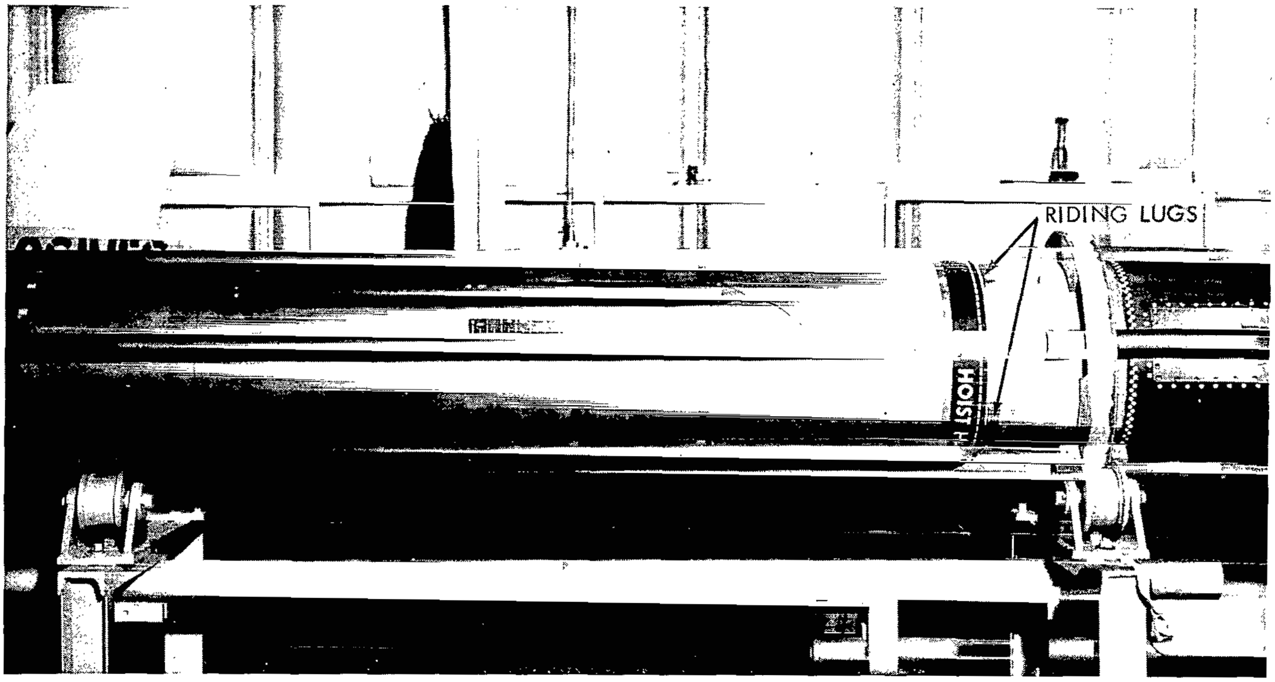

Figure 6—Portion of Aerobee Rocket showing forward riding lugs.

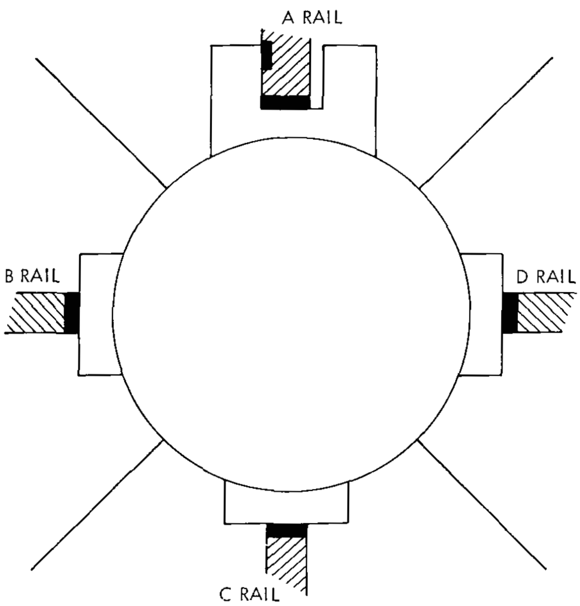

Figure 7—Aerobee 150A orientation in tower (looking up) and view of rail-guide lug contact points (shaded).

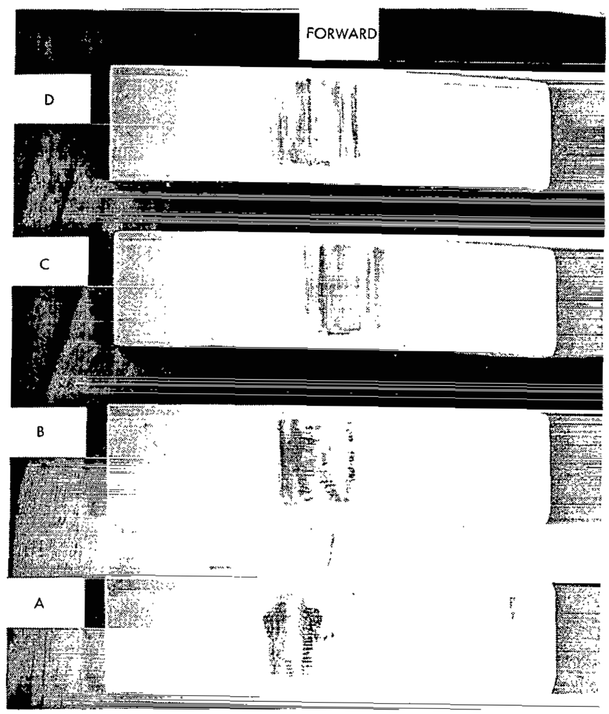

Figure 8—Replicas of NASA forward rocket riding lugs.

FLIGHT TIME HISTORY

The major vehicle flight parameters and event times for NASA 4.20 and NASA 4.68 tests are presented in Table 1. It is appropriate to briefly discuss the flight time history of Aerobee as a reference for the flight vibration data. For high initial thrust, the booster is fired first by remote control. The firing signal causes the overboard dump valve, incorporated in the pressure regulator valve, to be closed by a squib-activated piston located just aft of the attitude control system. This is the first event sensed by the vibration pickups. A microswitch senses this arming and completes circuitry to ignite the booster. As the vehicle moves vertically by initial booster thrust, it pulls away from a trip wire anchored to the launching tower. Resultant pulling of the trip wire initiates the sequence of events for sustainer ignition.

INSTRUMENTATION

NASA 4.20 Aerobee Rocket

Two piezoelectric transducers were installed on the aft side of the attitude control system (ACS) mounting plate at missile station 93 (Figures 10 and 11). One accelerometer was oriented longitudinally, along the thrust axis, the other, laterally along the B-D rail plane of the launch tower. Full deviation for the longitudinal channel was ±201 g's; for the lateral channel ±182 g's.

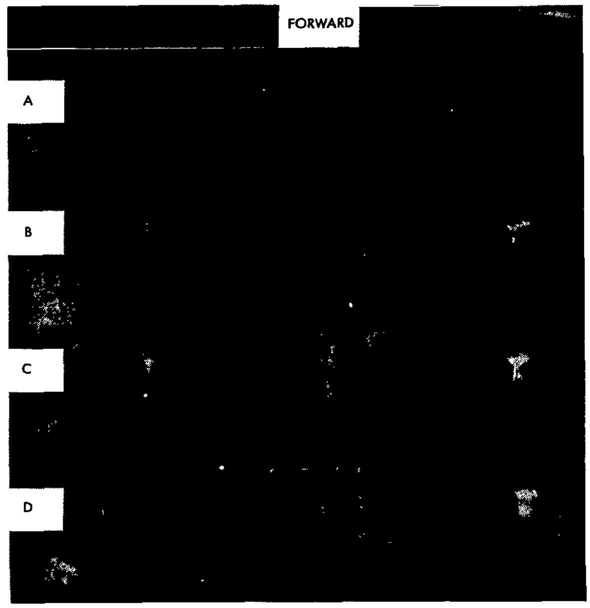

Figure 9—Replicas of NASA aft rocket riding lugs.

Table 1

Vehicle Flight Parameters and Event Times; Liftoff; t = 0 sec.

Event	Time (Sec)	
	NASA 4.20	NASA 4.68
Squib Firing	-0.3	-0.3
Liftoff	0.0	0.0
Booster Explosion	2.0	-
Hanger Exit	0.75*	0.78
Tower Exit	1.1*	1.1*
Booster Burnout	-	2.5*
Maximum Q	18.0*	19.0*
Rocket Burnout	52.0*	52.0*

*Approximate times.

The accelerometer signals were conditioned utilizing "charge" amplifiers and filter-clipper-bias units. The conditioned signals were then fed into an FM/FM telemeter and transmitted to Wallop's ground station via a slot antenna in one of the rocket fins (Figure 5). Standard IRIG FM/FM telemetry was used with the longitudinal accelerations transmitted on channel E (70 kc, ±15%) and the lateral accelerations transmitted on channel 16 (40 kc, ±7-1/2%). The frequency response, typical for both channels, is shown in Figure 12.

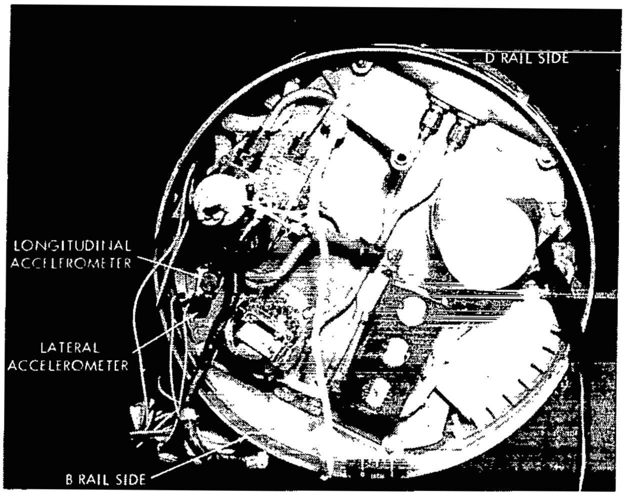

Figure 10–NASA 4.20 ACS, rear view.

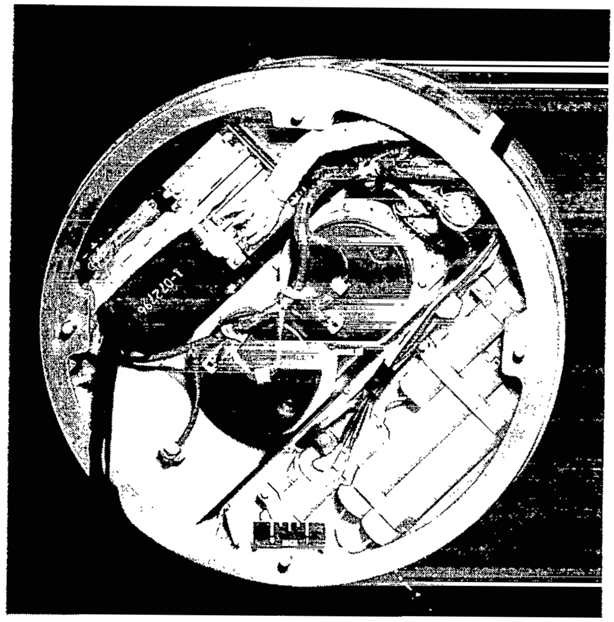

Figure 11–NASA 4.20 ACS, front view.

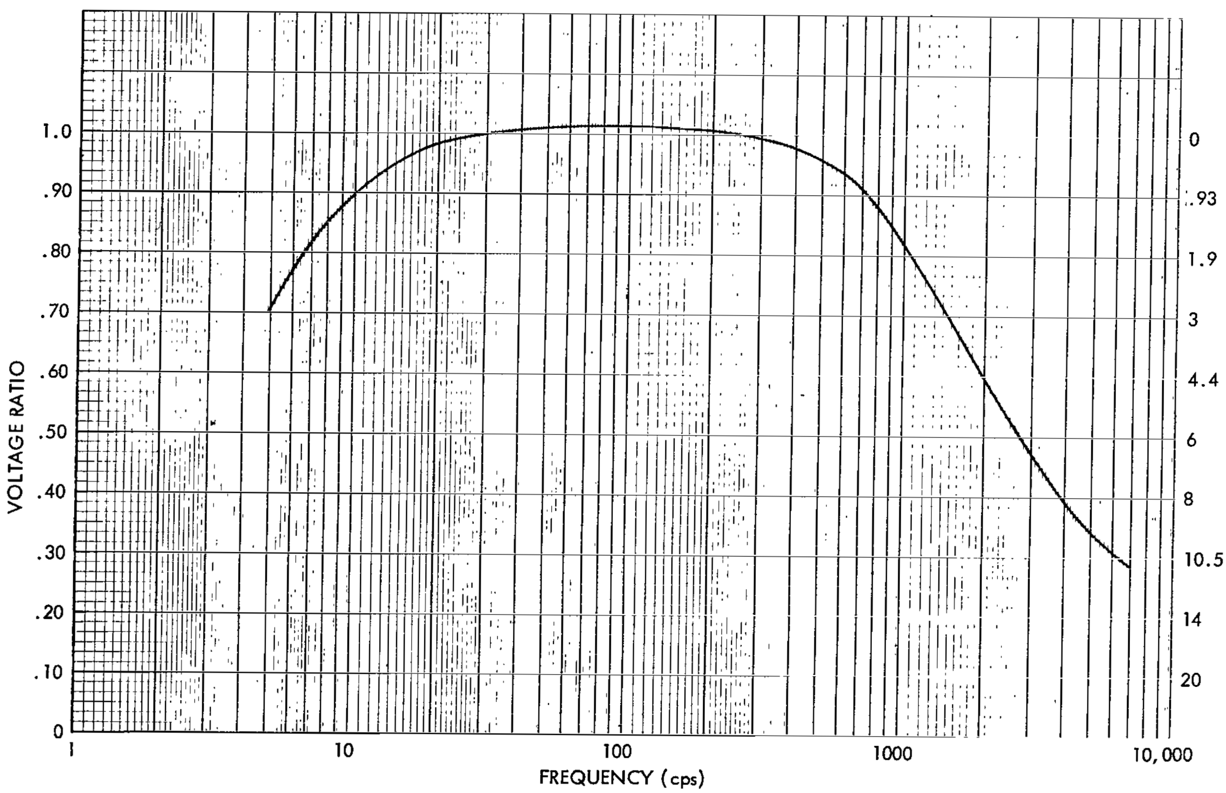

Figure 12–Typical system frequency response for all channels, NASA 4.20, NASA 4.68.

NASA 4.68 Aerobee Rocket

Two piezoelectric transducers were installed on the aft side of the ACS mounting plate at MS 93. The accelerometer mounting block plate is shown in Figure 13. The orientation of the transducers was approximately the same as for NASA 4.20; however, modifications to the ACS obviated exact replication of the mounting block location. A front view of the NASA 4.68 ACS, (Figure 14), is included for comparison of the modifications. In addition, a third transducer was mounted on the base of the instrumentation rack at MS 87 and oriented laterally along the A-C rail plane. Full deviation for all three channels was ±40 g's. IRIG letter channels E, C, and A (±15% deviation) were used in the FM/FM system. Longitudinal axis vibrations (MS 93) were measured on channel C, the lateral axis vibrations (MS 93) were measured on channel E, and the lateral axis vibrations (MS 87) were measured on channel A. The frequency response, typical for these channels is shown in Figure 12.

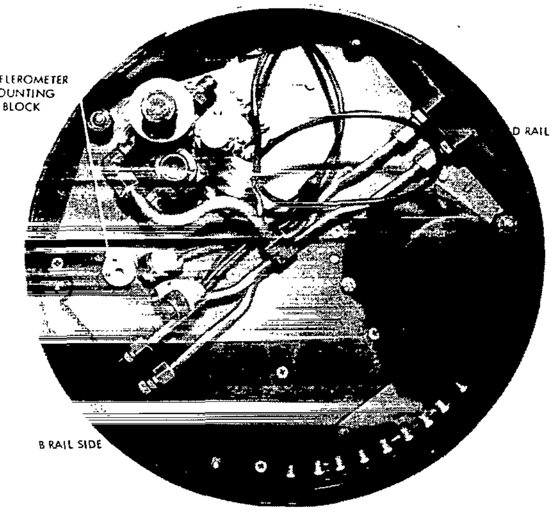

Figure 13—NASA 4.68, ACS, rear view.

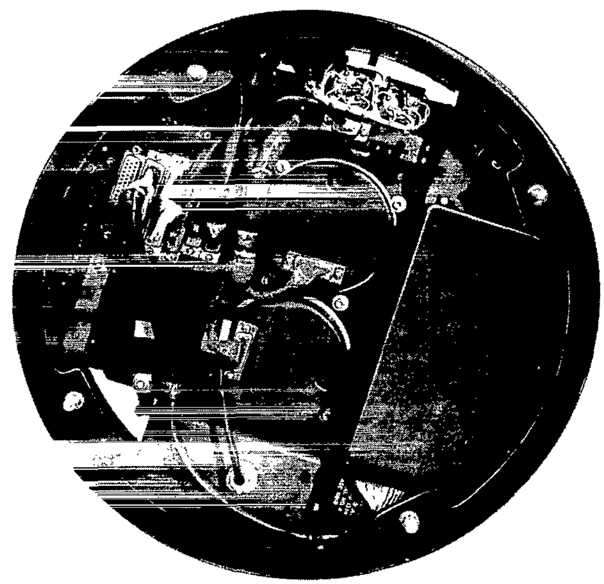

Figure 14—NASA 4.68, ACS, front view.

In addition to the in-flight instrumentation, the tower was instrumented with a microswitch at the 85-foot level to determine booster exit time from the building; a microphone to determine the airborne noise level inside the building; and accelerometers on rails A (tangential), B and C (radial) at the 85-foot level to determine rail shock and vibration levels. Full deviation for the microphone channel was 167 db; for the accelerometer channels, ±50 g's. The frequency response of the tower instrumentation was essentially flat to 10 kc. Just prior to the launch, a blue dye was sprayed on the rails for visual indication of lug contact.

DATA REDUCTION

A block diagram of the data reduction system is shown in Figure 15. Although not included in the system, additional equipment was used to inspect the subcarriers for relative amplitude, intermodulation noise level, and frequency drift to insure the validity of the data. Data reduction consisted of rms vibration levels versus time plots, instantaneous acceleration versus time plots and frequency versus time plots. The flight system frequency response was equalized from 0.2 kc to 3.0 kc prior to the data reduction. The low-pass output filters (LPOF) used are noted on the individual displays.

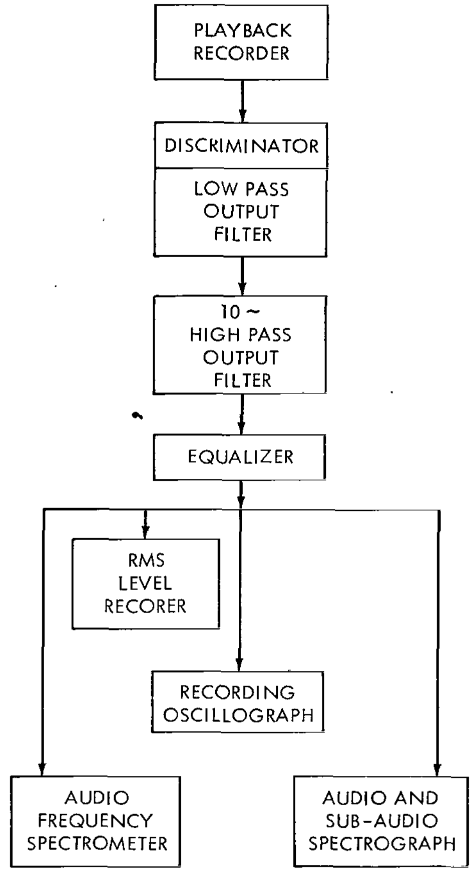

Figure 15—Data reduction system.

TEST RESULTS

NASA 4.20 Aerobee Rocket

An irregularity occurred when the booster exploded approximately 2.0 seconds after lift-off. The rocket survived the explosion and continued to function except that the roll rate was 3.0 rps instead of the expected 2.0 rps, and that the rocket evidently experienced a resonance due to the explosion.

Because the flight was not considered representative, data analyses were restricted to the time period from lift-off through booster explosion with the exception of the RMS vibration time histories. These are shown for the longitudinal and lateral axes in Figures 16 and 17 respectively. The abscissa (time) is linear; each division on the ordinate (amplitude) represents one db. Vibration transients are indicated at squib firing, lift-off, booster explosion, and rocket motor burnout in both axes. The highest vibration levels occurred between lift-off and hanger exit. During this period the average levels were approximately 7 g's RMS in both axes.

Instantaneous acceleration versus time records for the period from T - 0.4 seconds to T + 2.2 seconds are shown in Figure 18. The display is linear with respect to both acceleration level and time. Maximum amplitudes measured during lift-off and booster explosion were 22 g-pk and 29 g-pk respectively in the longitudinal axis; 24 g-pk and 44 g-pk in the lateral axis.

In view of the short time duration (0.7 seconds) of the high level vibration, quantitative spectral analyses were considered unwarranted. However, for indications of the spectra, an audio spectrograph having a 20 cps band pass filter is displayed (Figure 19). The display is a frequency versus time characteristic and is linear with respect to both parameters. The relative vibratory level is indicated by the shading between grey and black; black indicating the higher level. In the longitudinal axis, the bursts during the closed tower portion of flight and during booster explosion appears to be random. The predominate frequency was approximately 1350 cps and occurred during

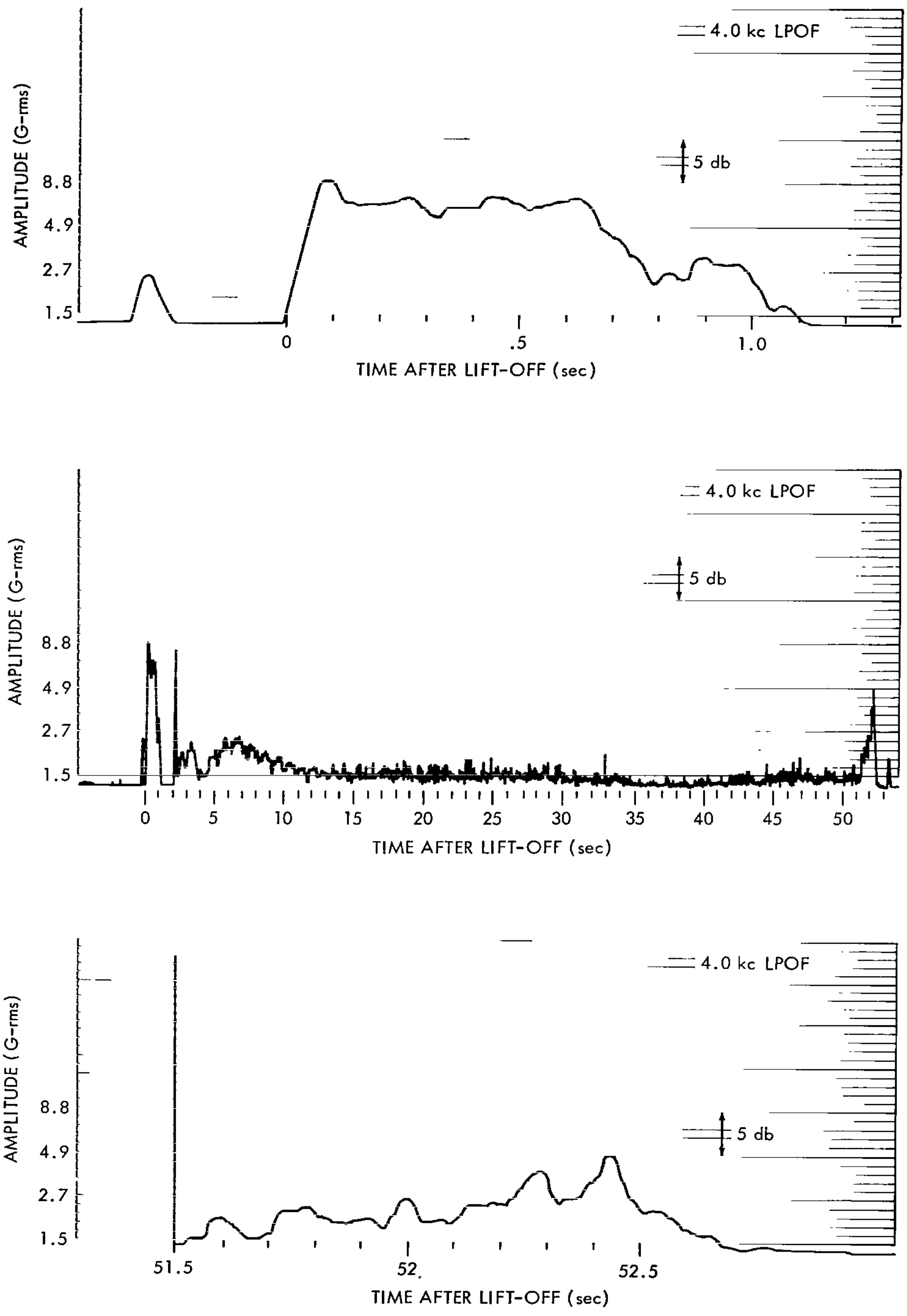

Figure 16–Vibration time history NASA 4.20, ACS longitudinal.

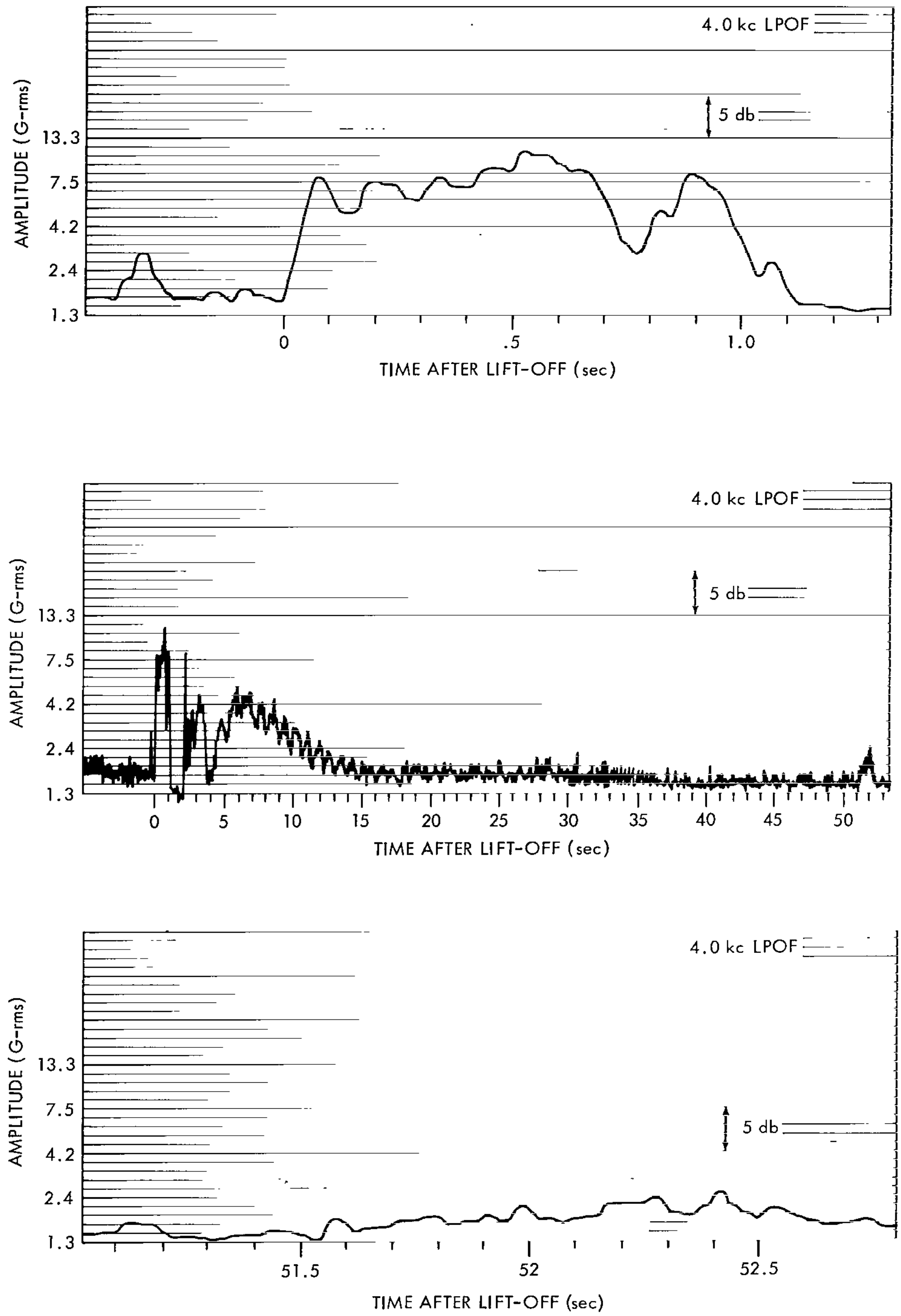

Figure 17–Vibration time history NASA 4.20, ACS lateral.

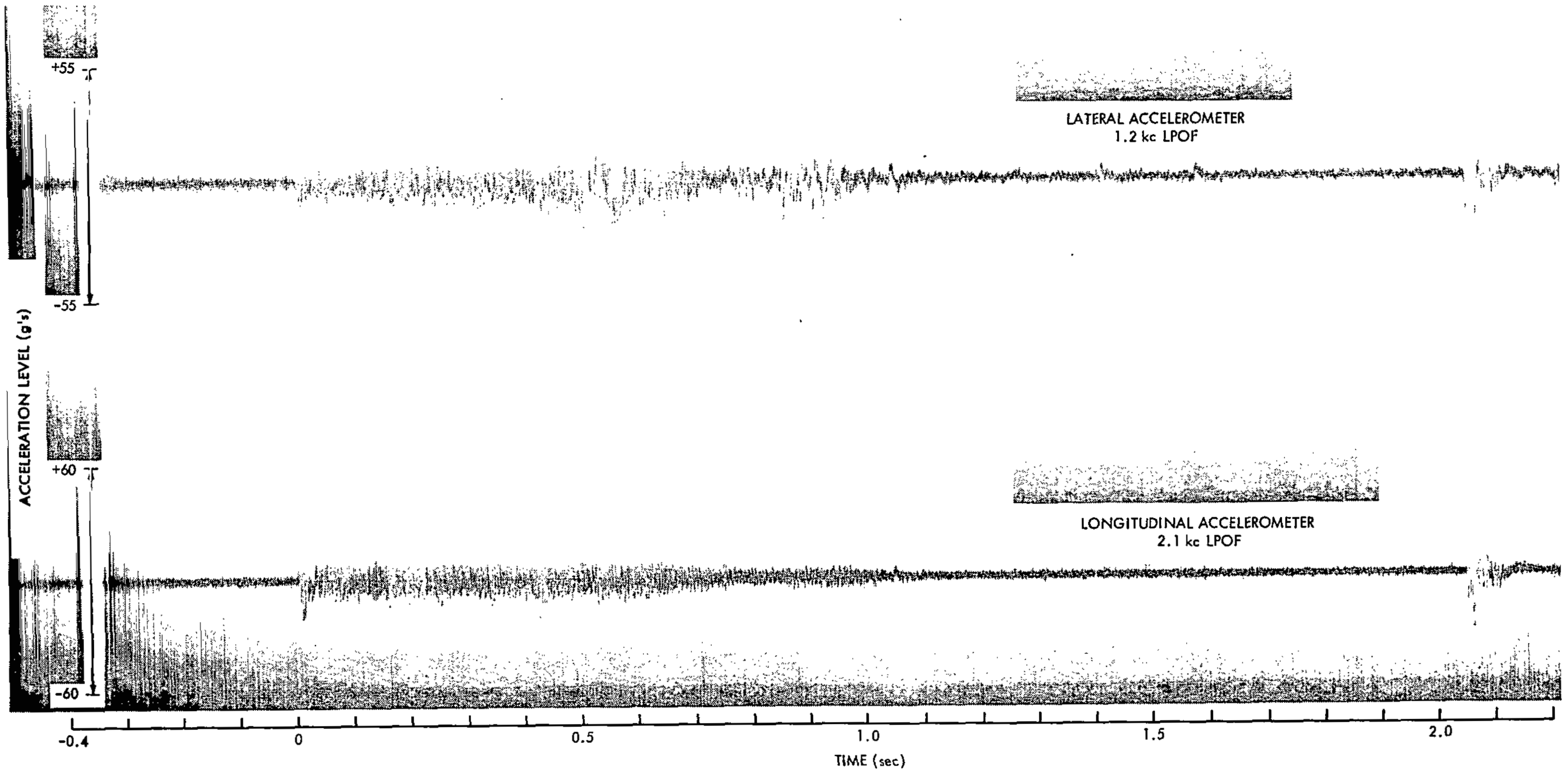

Figure 18—NASA 4.20 vibration at liftoff.

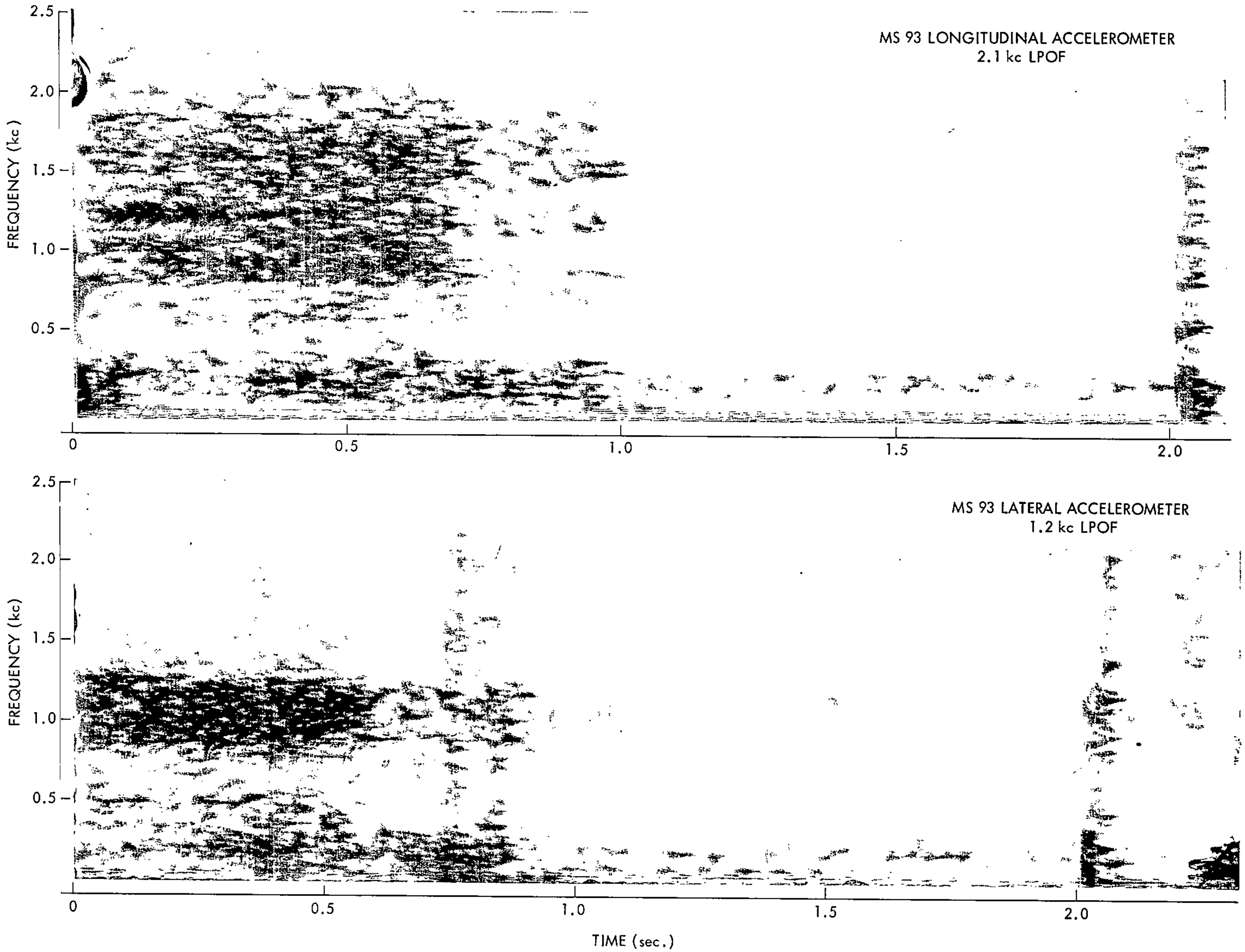

Figure 19–NASA 4.20 launch history.

the former. In the lateral axis, the most significant frequencies noted are in the 800 cps–1200 cps range; the upper limit being restricted by the low-pass output filter.

NASA 4.68 Aerobee Rocket

The trajectory and vehicle performance of this flight is considered to be typical for the Aerobee 150A rocket. The RMS vibration time histories for the longitudinal and lateral axes at MS 93 are shown in Figures 20 and 21 respectively. The first recorded event is the closing, by squib firing, of the overboard dump valve. Lift-off follows in approximately 0.3 seconds. During the period between lift-off and hanger exit, the average levels were approximately 7 g's RMS in both axes. The next significant event was a drop in RMS level at approximately +0.7 seconds. The microswitch installed at the 85 foot level indicated that the exit time was +0.78 seconds. From +0.7 seconds to tower exit at +1.1 seconds the levels drop, with the exception of peaks at hard impact, to very low levels. Comparison of Figures 16 and 17 with Figures 20 and 21 indicate similarity of vibration levels during the tower portion of both flights.

Proceeding on, the rocket enters the region of maximum dynamic pressure at approximately +19 seconds and the resultant slight increase in level is attributed to buffeting. Levels drop again until motor turbulence is experienced near burnout.

The third accelerometer located at MS 87 malfunctioned at launch. Investigation revealed that it was probably bi-stable and either became inoperative or experienced a drastic change in sensitivity due to shock. The trouble was attributed to an improper manufacturing process.

The overall sound pressure level (uncorrected) versus time measured by the tower microphone is shown in Figure 22. It appears (from comparison of Figures 20 and 21 with Figure 22) that some amount of the rocket vibration (to +0.7 seconds) is due to acoustic coupling. The maximum sound pressure level measured during this time was approximately 146 db.

Instantaneous acceleration versus time plots for the period from -0.6 seconds to +2.2 seconds are presented in Figure 23 for the longitudinal and lateral axes at MS 93 and for the B rail radial accelerometer which was located at the 85-foot level. The sensitive axes of the lateral and B rail accelerometers were approximately parallel. Maximum values measured were 29 g-pk and 24 g-pk for the longitudinal and lateral accelerometers respectively. The B rail experienced accelerations greater than 50 g-pk for approximately 0.3 seconds; the measuring system was overloaded during this time period.

A plot of rail-lug contact as well as hard hits and joint hits is presented in Figure 24 (see also Table 2).

Rail inspection indicates that the rocket rides the rails rather smoothly during the first 88 feet of travel. This light and relatively smooth contact induces a vibratory motion, rather than shock impulse, to the rocket (Figure 23). Rail contacts inside the hanger were hard to distinguish while contacts outside the hanger were very noticeable and at some points the rails were gouged. As the rocket leaves the building, it appears that its velocity is such that it breaks free of the

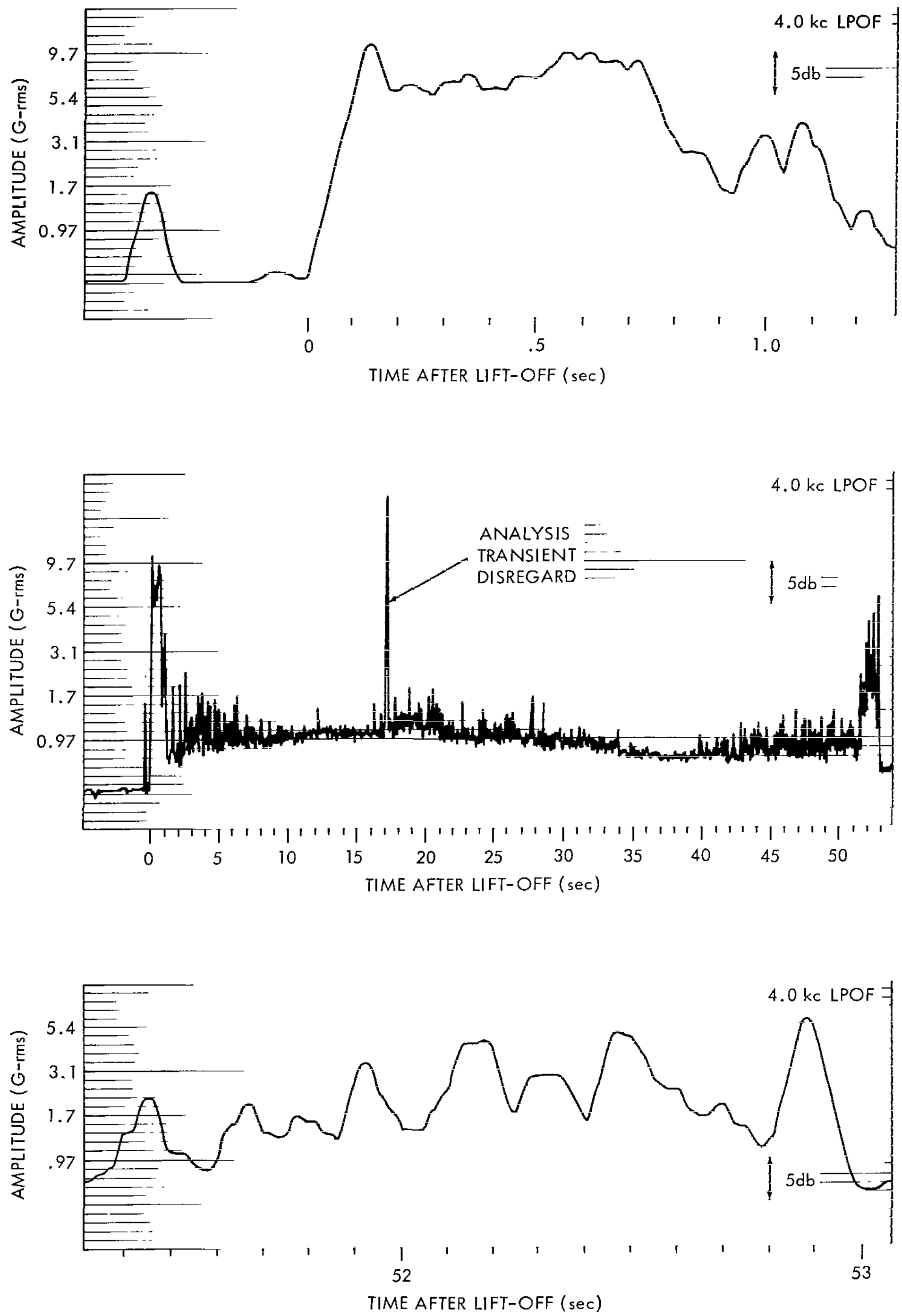

Figure 20—vibration time history, NASA 4.68, ACS longitudinal.

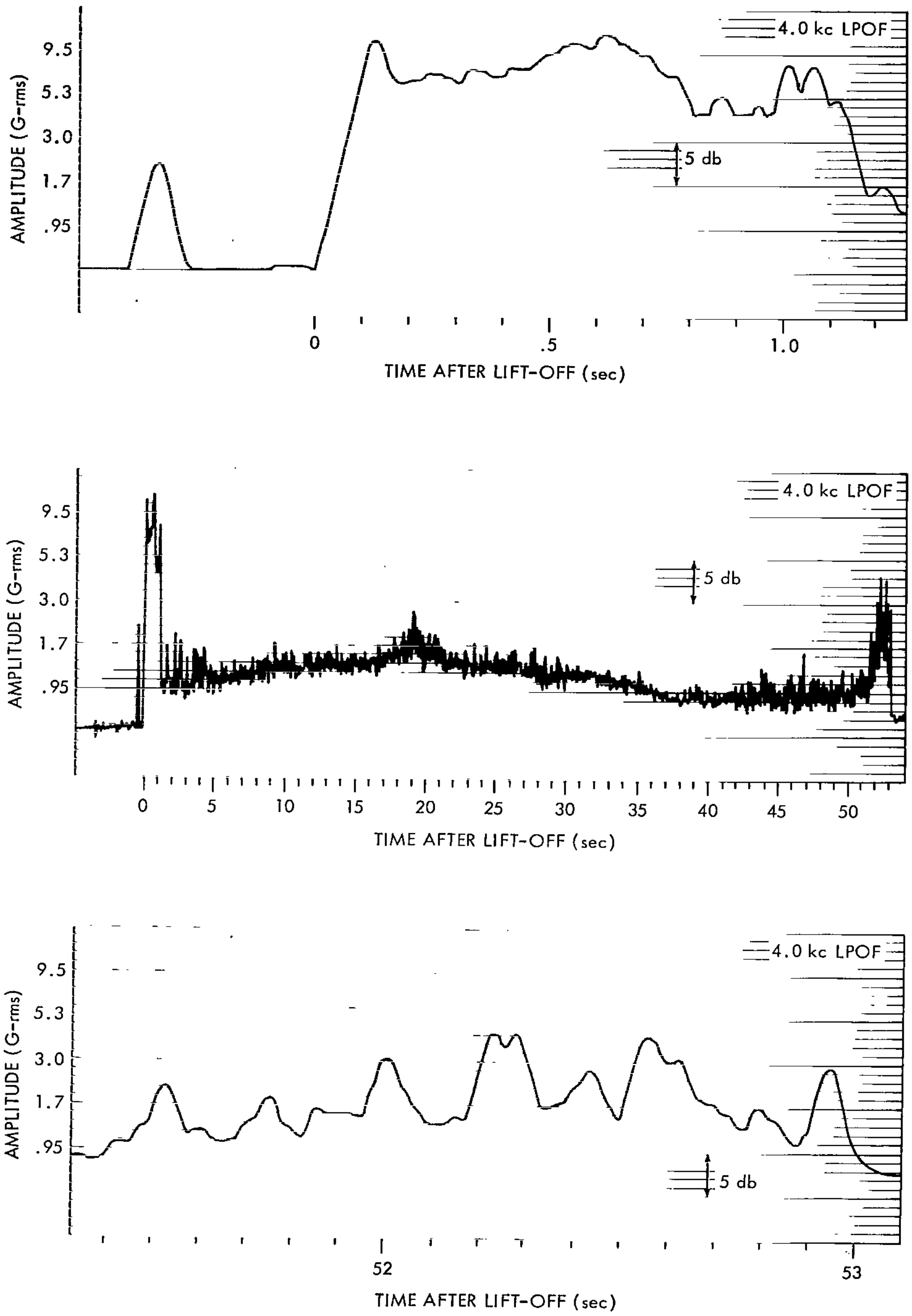

Figure 21—Vibration time history, NASA 4.68, ACS lateral.

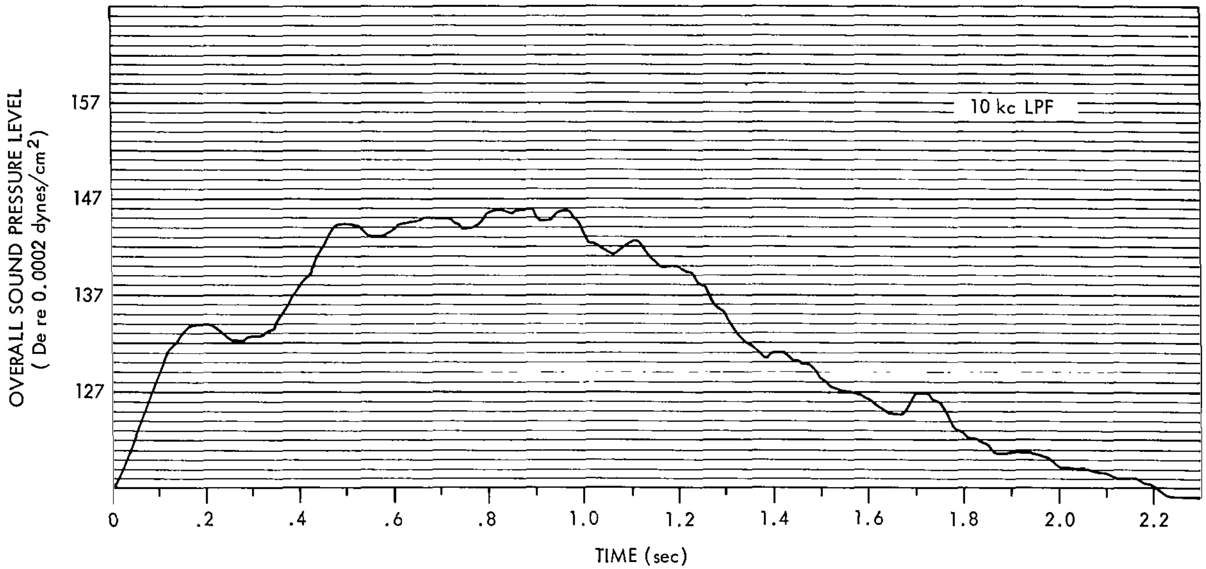

Figure 22—NASA 4.68 airborne sound pressure level versus time; tower microphone 10 kc.

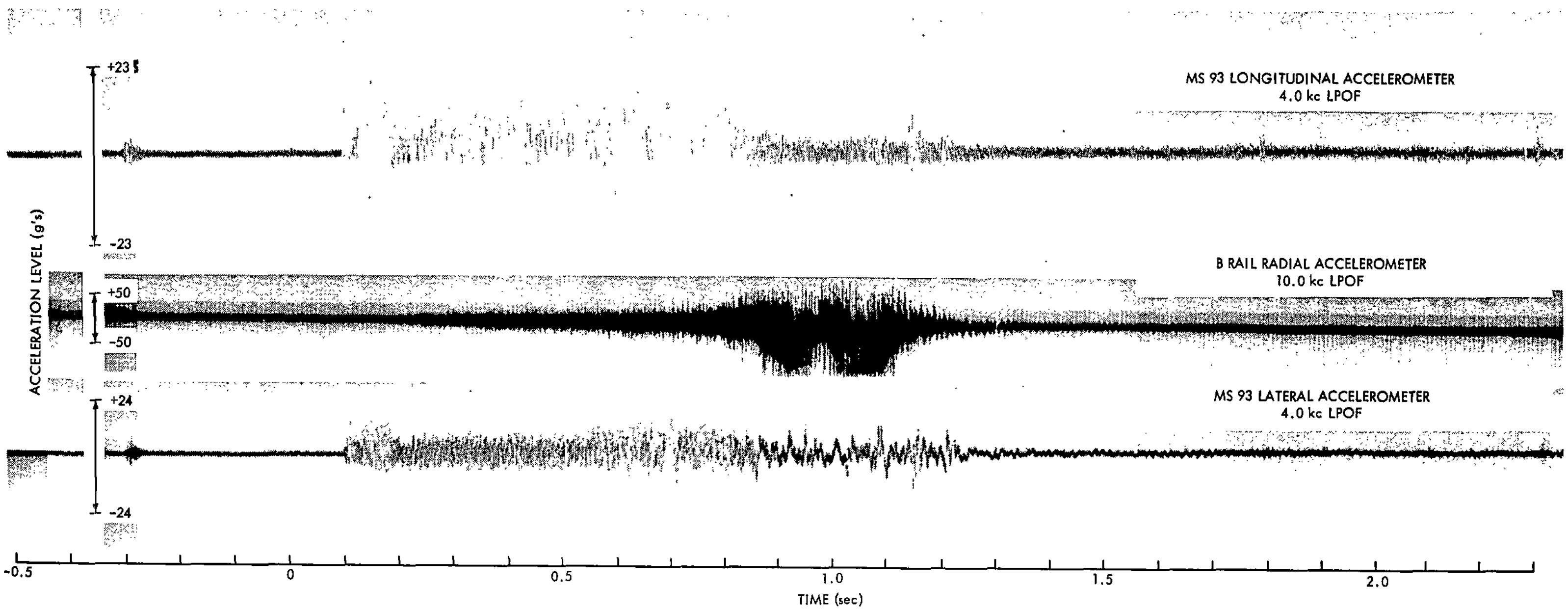

Figure 23—NASA 4.68 vibration at liftoff.

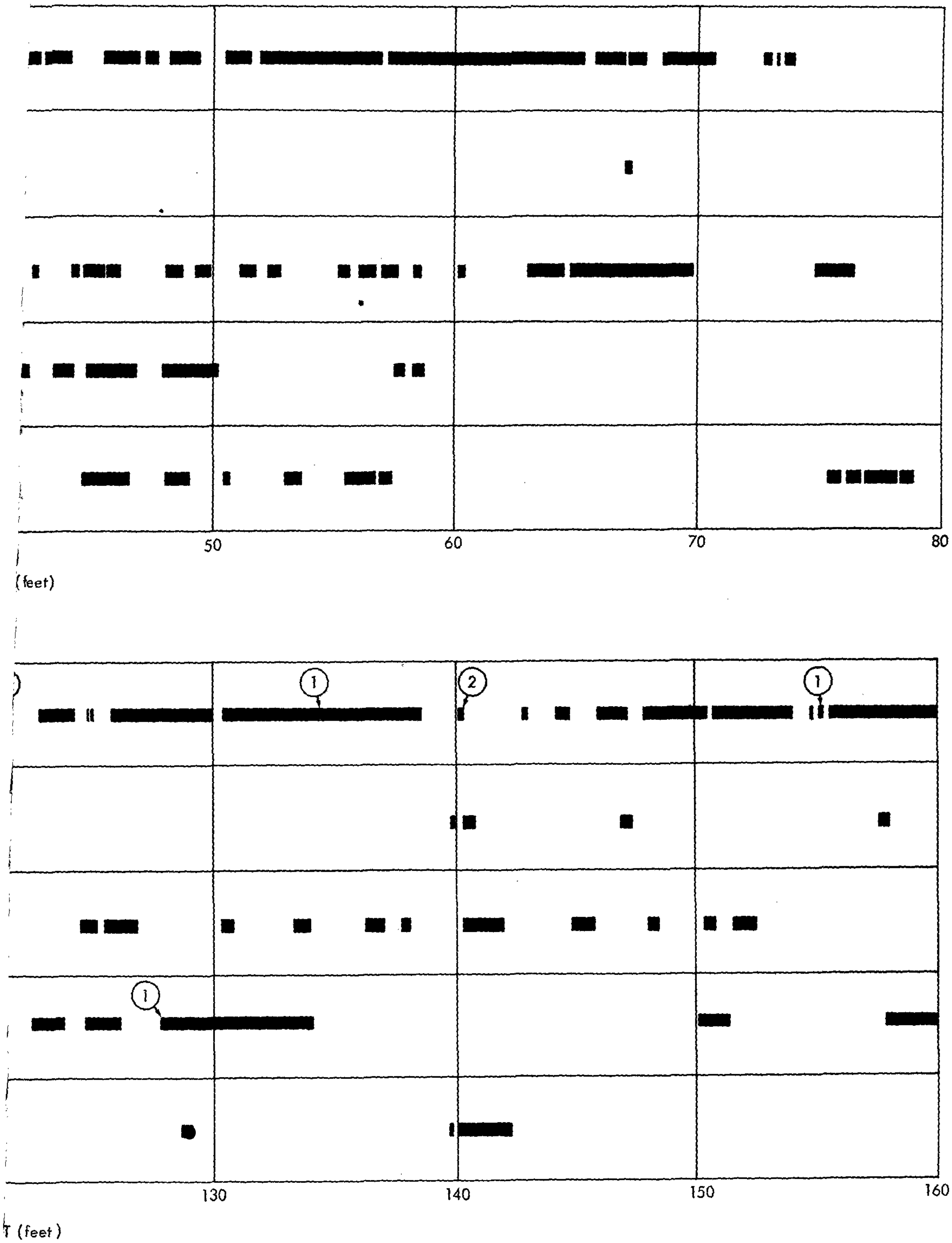

ring the
The low
; during the
re attributed
he rail

s due to the
spin. Note
ge contact.
booster
t, 4 inches

pectro-
ıt to per-
pectra for

:d-tower
'tion.
ıdes occur
.e fre-
burnout,
ıuencies

e data
ıeasured;
Photo-
n in Fig-

:ets. The
' than

ıils:
terference.

Figure 24–NASA 4.68 rail-lug contact.

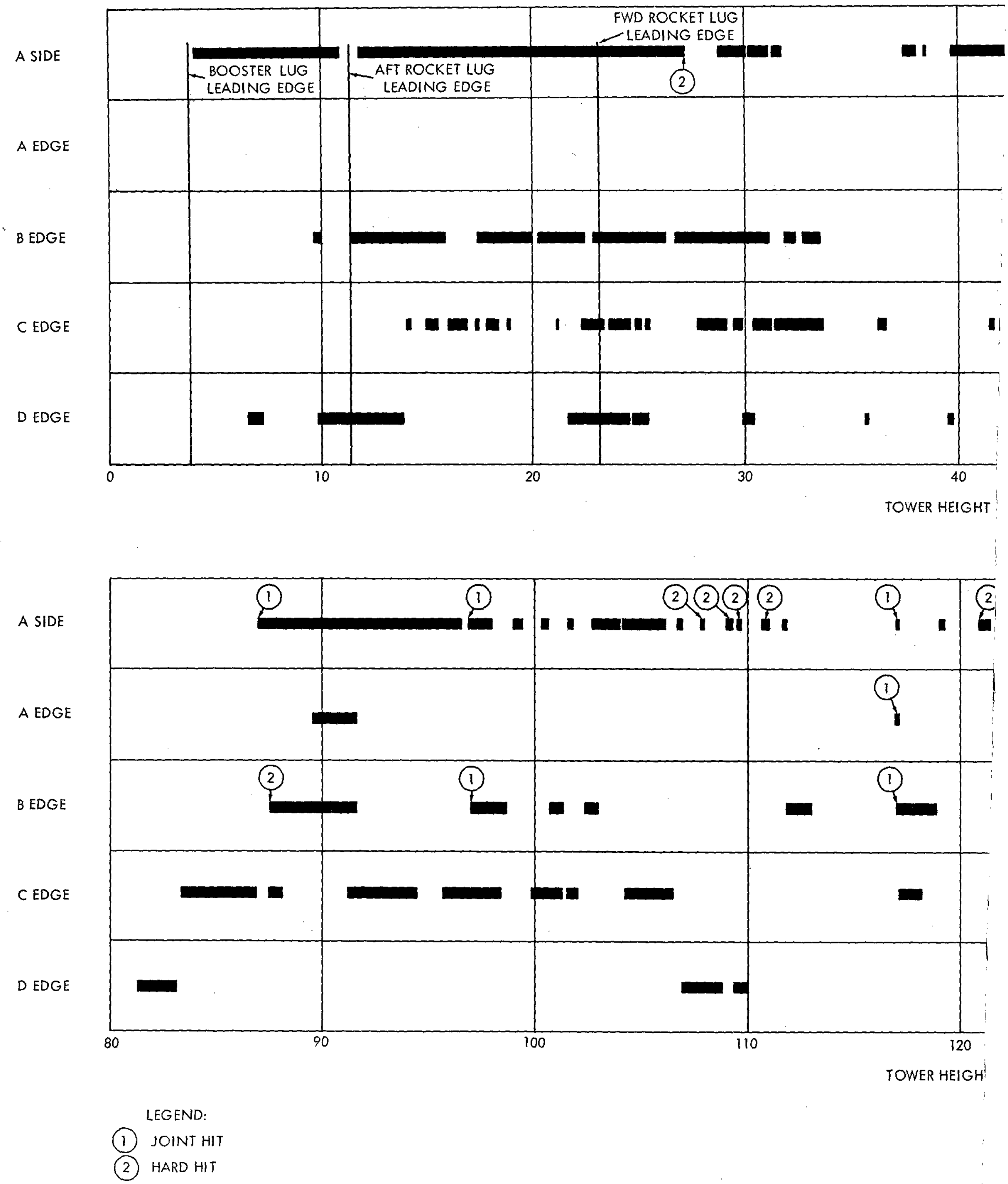
A SIDE
A EDGE
B EDGE
C EDGE
D EDGE
BOOSTER LUG LEADING EDGE
AFT ROCKET LUG LEADING EDGE
FWD ROCKET LUG LEADING EDGE
0
10
20
30
40
TOWER HEIGHT
80
90
100
110
120
TOWER HEIGH
LEGEND:
1 JOINT HIT
2 HARD HIT

Table 2

Percentage of Rail-Lug Contact.

Contact	Rail				
	A Side	A Edge	B Edge	C Edge	D Edge
In-hanger	36.9%	0 %	22.6%	13.6%	13.6%
Out-of-hanger	29.8%	2.4%	12.6%	17.8%	3.1%
Total	66.7%	2.4%	35.2%	31.4%	16.7%

rails and starts to impact during the open tower portion of flight. The low frequency lateral oscillations during the open tower portion of flight are attributed to the vehicle's response to the rail impacts.

The A rail side contact is due to the booster guide lug restraining spin. Note the small amount of A rail edge contact. At two points on the side of the A rail, welds were not ground flat, thus obstructing the booster guide lug, and were severely gouged. Two rail joints, located at tower heights of 27 feet, 4 inches and 87 feet, 11 inches, were out of line and gouged by the side of the booster guide lug.

Qualitative spectral analyses of the vibration data were performed using an audio spectrograph with a 20 cps bandwidth filter. The gain setting for each channel was held constant to permit comparison of amplitude variation with time. Lift-off, max Q, and rocket-burnout spectra for both MS 93 axes are shown in Figures 25, 26, and 27, respectively.

In both axes, the vibratory spectrum is relatively broad and intense during the closed-tower portion of flight, followed by a series of shock-type pulsations during the open-tower portion. During the time that the vehicle passes through the region of max Q, the greatest amplitudes occur in the frequency bands of 175-200 cps and 900-1100 cps in the longitudinal axis; and in the frequency bands of 175-200 cps and 1500-1800 cps in the lateral axis. During rocket motor burnout, the vehicle again experiences a series of shock-type pulsations with the predominant frequencies less than 300 cps in both axes.

One-third octave analyses of the MS 93 accelerometer data and the tower microphone data were then performed. The maximum levels occurring within 0.1 second intervals were measured; the values which were above the ambient noise level are presented in Tables 3, 4, and 5. Photographs of the three-dimensional models constructed from the resulting records are shown in Figures 28 through 33.

CONCLUSIONS AND RECOMMENDATIONS

Similar vibration data have been obtained from two flights of Aerobee 150A 4-fin rockets. The maximum levels occurred during the in-tower portion of flight and are considerably lower than those reported for the 3-fin Aerobees.

The following recommendations are made, based on visual examination of the tower rails:

1. All rail joints should be inspected for misalignment prior to flight to avoid joint interference.

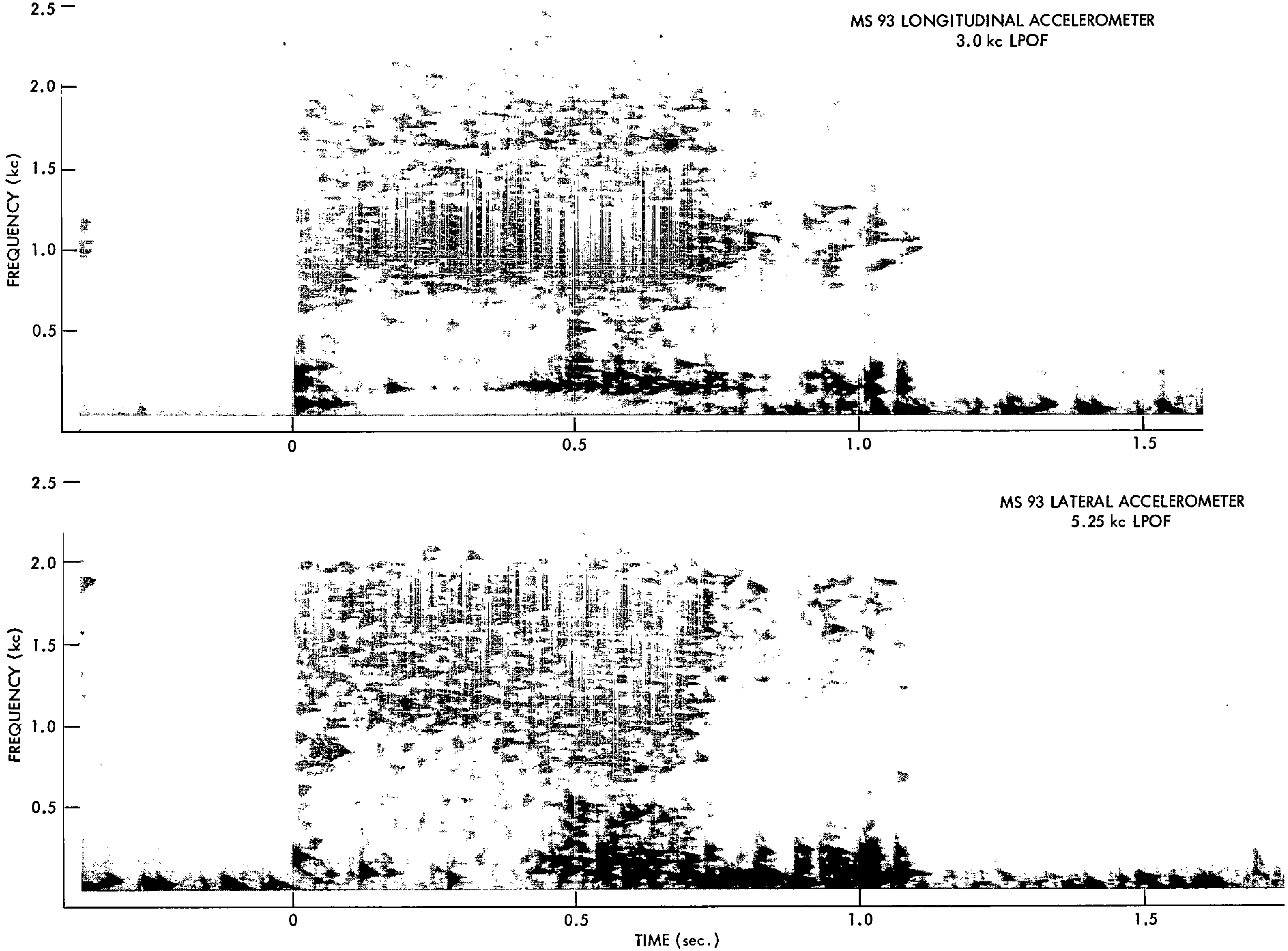

Figure 25–NASA 4.68 launch history.

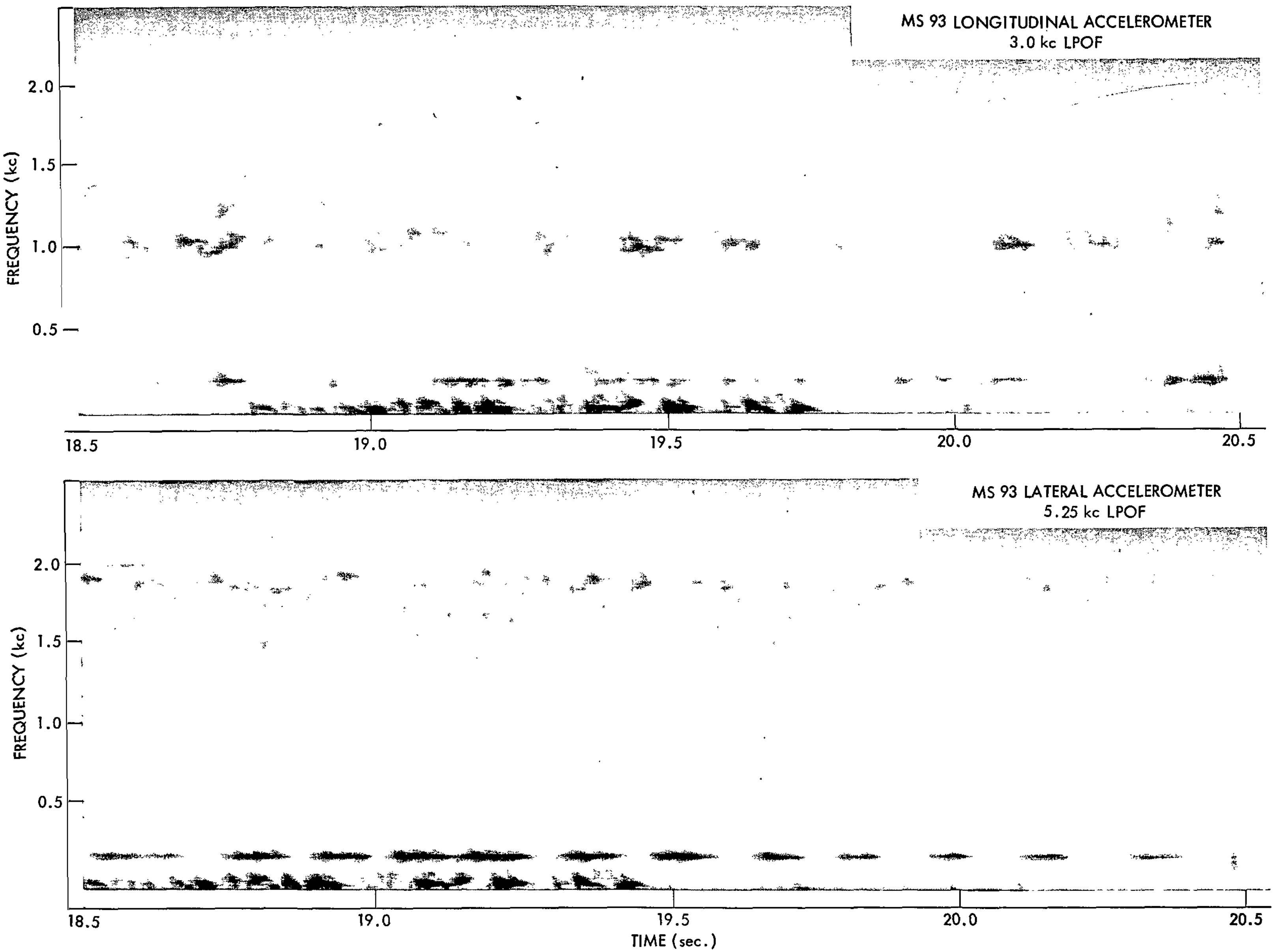

Figure 26–NASA 4.68 max Q history.

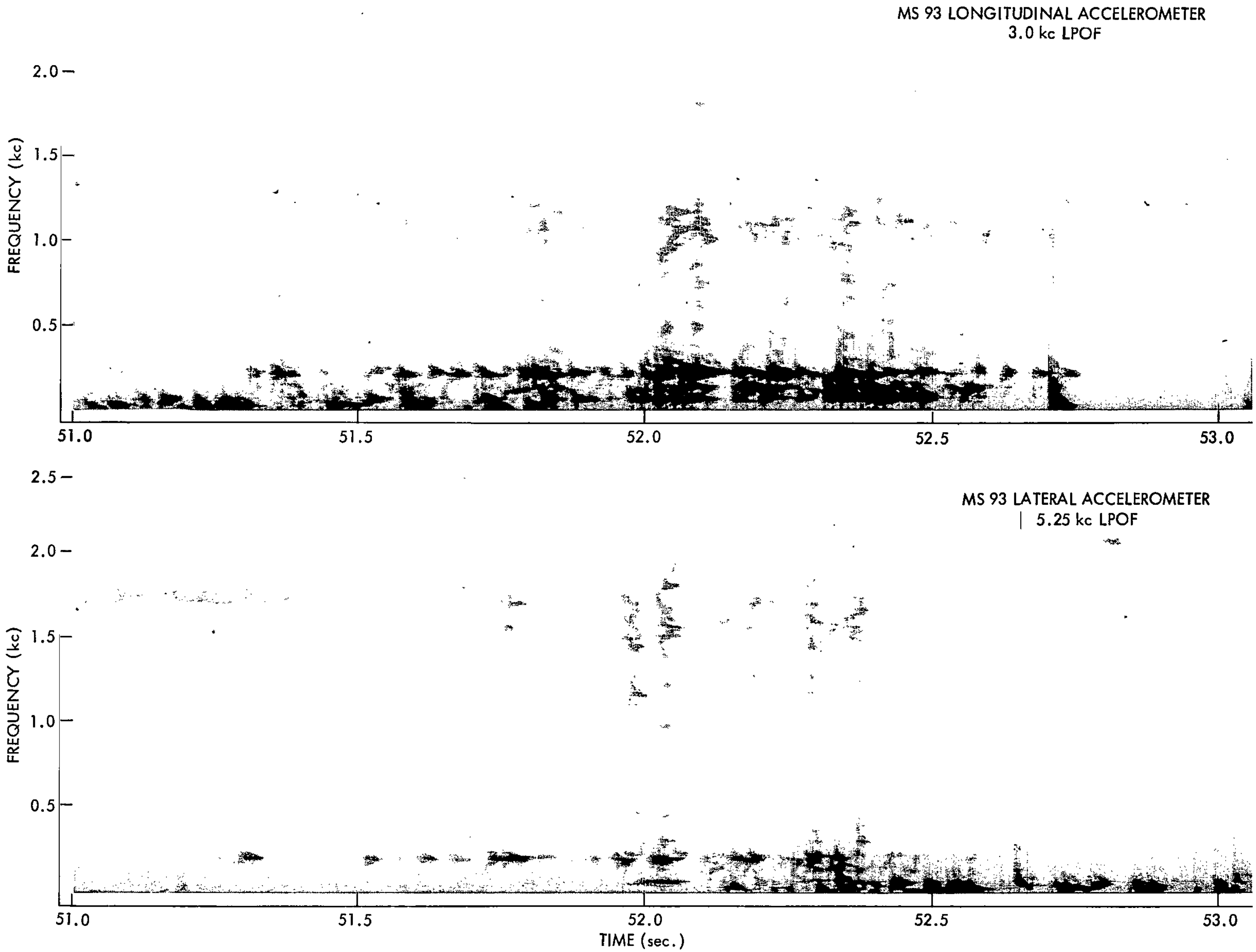

Figure 27–NASA 4.68 rocket burnout history.

Table 3

NASA 4.68 Launch Vibratory Acceleration Longitudinal Axis.
One-Third Octave Band Analysis, 4.0 kc LPOF.

Center Frequency (cps)	Maximum Acceleration (g-rms) from t to t + 0.1 Seconds																	
	t = 0	0.1	0.2	0.3	0.4	0.5	0.6	0.7	0.8	0.9	1.0	1.1	1.2	1.3	1.4	1.5	1.6	1.7
40	0.6	0.3							0.3									
50	0.8	0.4																
63	1.1	1.1										0.4						
80	1.6	1.6	0.3				0.6	0.5	0.3			0.5	0.4					
100	0.7	0.4			0.4	0.5	0.5		0.5	0.4	0.5	0.5						
125	0.4	0.4				0.7	0.6	0.5	0.5	0.6	1.0	0.6						
160	1.1	0.9	1.3	0.6	1.6	2.3	1.4	1.4	1.1	1.1	2.2	2.2	1.2					
200	1.6	1.6	1.0	0.4	2.4	2.5	1.9	1.9	1.2	0.8	1.5	1.1	0.5	0.3	0.3		0.4	0.4
250	1.3	1.1	0.4	0.6	0.6	2.3	1.7	1.0	1.4	1.2	1.2	1.6	0.4	0.5	0.7	0.7	0.7	0.6
315	1.5	1.1	0.7	0.8	1.2	2.6	1.3	1.2	0.5	0.7	1.1	1.2	0.5	0.4	0.4	0.5	0.4	0.5
400	0.8	0.6	0.6	0.5	0.8	1.4	0.8	0.7	0.6	0.4	0.4	0.5						
500	0.9	0.8	1.0	0.8	1.0	1.6	1.8	0.8	0.6	0.4	0.4							
630	1.5	1.5	1.1	1.1	1.3	1.8	1.4	1.1	0.8	0.5	0.7	0.7						
800	1.8	5.0	2.1	3.3	2.7	5.4	4.6	3.5	1.2	1.0	1.5	1.1	0.4	0.4	0.4	0.4	0.4	0.5
1000	1.8	5.2	7.1	7.1	6.9	8.7	9.4	8.4	2.4	2.2	2.2	2.1	0.6	0.4	0.4	0.4	0.6	0.6
1250	1.8	4.4	4.5	5.0	4.3	6.8	6.2	6.6	2.1	1.8	2.0	2.0	0.6	0.4	0.4	0.4	0.4	0.5
1600	1.9	2.8	3.2	2.8	3.5	3.5	4.4	3.2	1.2	1.0	1.0	1.0	0.3					0.6
2000	2.2	2.5	3.1	2.7	3.0	2.8	3.5	2.9	1.3	1.1	1.3	0.9	0.6					
2500	1.4	1.4	1.9	1.7	2.1	1.6	2.2	1.2	0.8	0.6	0.5	0.4	0.5					
3150	1.1	1.1	1.5	1.4	1.8	1.1	1.5	0.9	0.6	0.6	0.6	0.6	0.8	0.3			0.4	1.0
4000	0.6	0.6	0.8	0.7	1.1	0.7	0.8	0.5	0.4	0.4	0.4	0.5	0.6					0.7

Table 4

NASA 4.68 Launch Vibratory Acceleration Lateral Axis.
One-Third Octave Band Analysis, 4.0 kc LPOF.

Center Frequency (cps)	Maximum Acceleration (g-rms) from t to t + 0.1 Seconds																	
	t = 0	0.1	0.2	0.3	0.4	0.5	0.6	0.7	0.8	0.9	1.0	1.1	1.2	1.3	1.4	1.5	1.6	1.7
40	0.7	0.4	1.2	1.0	1.1	1.1	1.7	4.7	3.8	4.8	4.8	0.7	0.5	0.4				
50	0.6	0.5	0.8	0.6	1.0	1.4	2.1	1.6	1.2	1.7	1.9	0.9						
63	0.5	0.6	0.5	0.5	0.6	2.0	2.8	1.0	2.3	1.2	4.5	3.8	0.7	0.6	0.5	0.5	0.4	0.3
80	0.9	1.1	1.1	1.2	0.7	1.9	4.7	1.7	1.7	1.5	4.6	3.4	0.7	0.4	0.5	0.6	0.6	
100	1.1	1.5	0.8	0.8	1.0	2.5	2.6	1.3	2.9	2.2	1.5	3.4	1.1	0.4	0.3	0.3	0.5	0.8
125	0.5	1.5	1.0	0.6	1.0	1.7	1.5	1.3	1.5	2.2	2.6	1.7	1.1					
160	1.0	1.2	1.1	0.9	1.2	3.0	3.8	7.4	1.0	1.7	3.2	3.2	0.4					
200	1.2	1.0	0.7	0.9	2.3	2.7	2.8	1.7	1.7	1.5	3.4	3.4						
250	1.0	0.7	0.5	0.9	1.0	2.4	2.4	1.5	1.3	2.0	2.7	3.0	0.3	0.4			0.5	0.5
315	1.2	1.0	1.0	0.9	1.3	2.1	1.7	1.8	0.8	1.2	1.2	1.0	0.3	0.7	0.5	0.5	0.6	0.6
400	1.0	1.0	1.3	1.0	1.0	2.6	2.0	1.8	1.4	1.0	1.0	0.8						
500	1.1	1.0	1.0	1.2	1.2	3.4	3.1	1.7	0.7	0.7	0.9	0.5						
630	1.2	1.2	1.2	1.3	1.5	1.8	2.1	1.1	0.8	0.4	1.1	1.4	0.4					
800	1.9	4.8	1.7	2.0	3.0	3.0	3.8	2.2	1.0	0.8	1.0	0.8	0.3					
1000	3.0	3.3	3.0	3.2	3.4	5.3	4.8	4.2	1.1	1.2	1.2	0.8						
1250	1.7	4.2	4.2	4.8	4.8	7.2	6.5	6.5	2.1	1.7	1.7	1.4	0.4	0.4	0.3	0.3	0.3	0.4
1600	3.0	6.8	6.6	7.8	9.1	9.1	11.7	7.9	3.3	3.5	3.6	2.5	0.6	0.6	0.7	0.6	0.6	0.7
2000	2.1	5.0	5.4	5.4	6.5	7.2	7.2	5.1	2.9	1.7	2.6	2.0	0.5	0.4	0.4	0.4	0.6	0.7
2500	1.6	1.6	1.1	1.3	1.3	1.7	2.2	1.3	1.0	0.8	0.7	0.7	0.6	0.4	0.4	0.3	0.6	0.9
3150	1.2	1.2	1.2	1.3	1.6	1.2	1.8	1.2	1.1	0.9	0.9	0.6	0.6	0.6	0.4	0.4	0.6	1.0
4000	0.6	0.7	0.6	0.6	1.3	0.7	0.9	0.5	0.8	0.6	0.5	0.7	0.6	0.4	0.4	0.4	0.5	0.9

Table 5

NASA 4.68 Airborne Sound Pressure Level (db) in Tower.
One-Third Octave Band Analysis, 10 kc LPF.

Center Frequency (cps)	Maximum Sound Pressure Level (db) from t to t + 0.1 Seconds																						
	t = 0	0.1	0.2	0.3	0.4	0.5	0.6	0.7	0.8	0.9	1.0	1.1	1.2	1.3	1.4	1.5	1.6	1.7	1.8	1.9	2.0	2.1	2.2	2.3
40						117	125	126	121	126	126	122												
50						119	123	121	127	124	127	124												
63						123	122	129	132	131	132	130	124											
80	117	118			121	125	125	123	128	131	131	124	124	121										
100		118	118		120	127	132	134	132	132	131	126	125	120	121	121								
125	117	120	119		124	125	133	131	137	140	132	130	132	125	120	118								
160	118	122	123	122	133	138	134	131	132	140	140	139	131	130	125	123	121	118						
200	121	123	122	122	134	136	133	132	136	135	135	128	132	131	124	119								
250	118	120	120	120	128	132	135	135	135	134	134	133	130	128	120	118	118	119	118					
315		120	124	122	129	136	136	137	137	136	133	135	133	128	124	123	118	121	119					
400	120	120	120	124	131	134	134	136	135	135	135	133	131	129	122	118		118						
500	119	122	123	123	132	135	133	135	135	134	131	131	129	123	123	120	117	117						
630	121	122	123	126	132	135	134	135	135	135	132	133	129	127	123	120								
800	122	122	123	126	131	134	135	135	135	134	134	133	129	125	119	119								
1000	120	124	126	126	131	132	134	135	133	133	133	131	127	122	122	119								
1250	120	124	125	127	128	131	133	134	134	132	132	128	124	123	117									
1600	119	121	122	124	127	130	133	131	130	130	125	122	118											
2000	120	121	121	124	127	128	131	131	131	130	127	124	120											
2500	117	119	119	123	127	127	127	125	122															
3150			118	120	124	125	127	127	127	126	124	119												
4000				119	121	124	124	124	122	121														
5000					118	121	123	123	123	120	119													
6300						120	121	121	120	119														
8000						118	118	118	118															

2. If it is desirable to further control the vibration during tower flight or if newer vehicles are designed for this tower, it is suggested that a thorough analysis of launch tower dynamics be made. In view of the deep gouges in the rails, some attention should be given to the design of the riding lugs and their supporting structure and the fore and aft location and number of lugs.

(Manuscript received October 4, 1963)

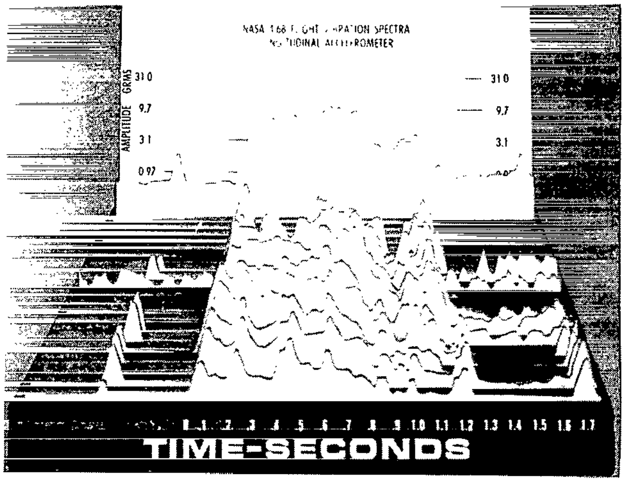

Figure 28—Front view of the three-dimensional plot of the NASA 4.68 overall acceleration and one-third octave analysis—longitudinal accelerometer 4.0 kc LPOF.

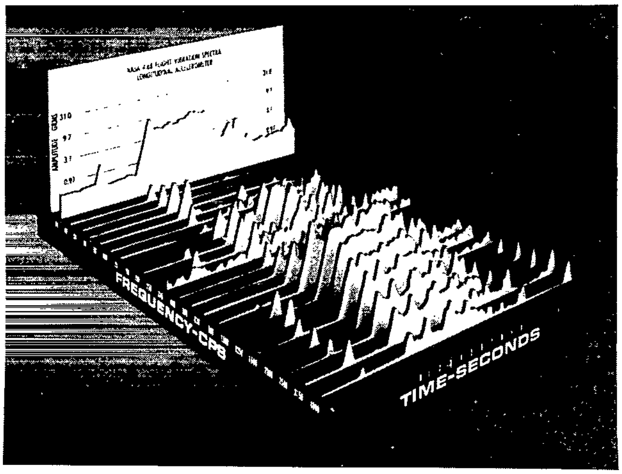

Figure 29—Left oblique view of the three-dimensional plot of NASA 4.68 overall acceleration and one-third octave analysis—longitudinal accelerometer 4.0 kc LPOF.

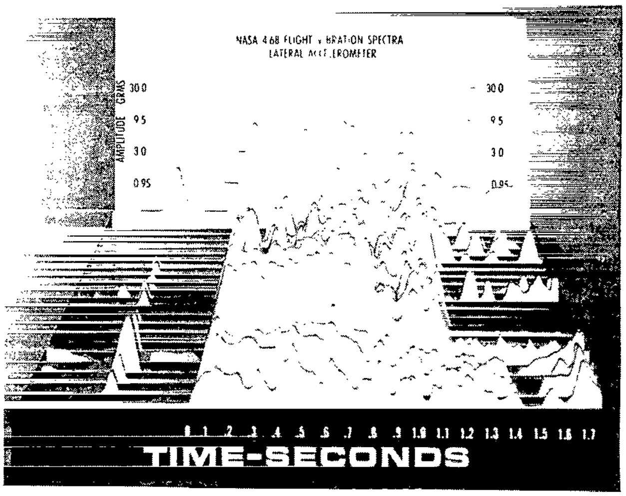

Figure 30—Front view of the three-dimensional plot of NASA 4.68 overall acceleration and one-third octave analysis—lateral accelerometer 4.0 kc LPOF.

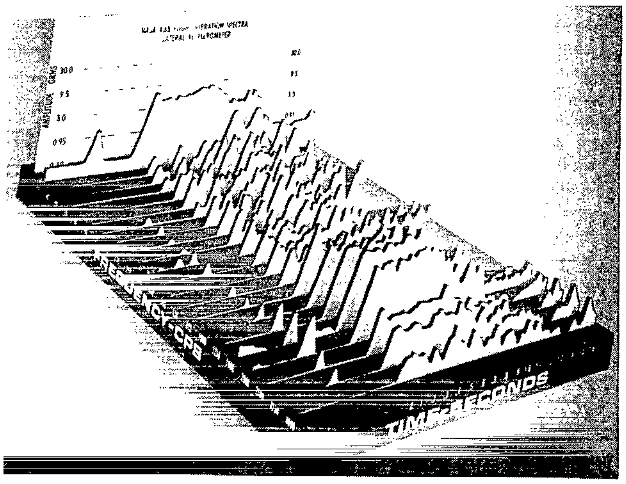

Figure 31—Left oblique view of the three-dimensional plot of NASA 4.68 overall acceleration level and one-third octave analysis—lateral accelerometer 4.0 kc LPOF.

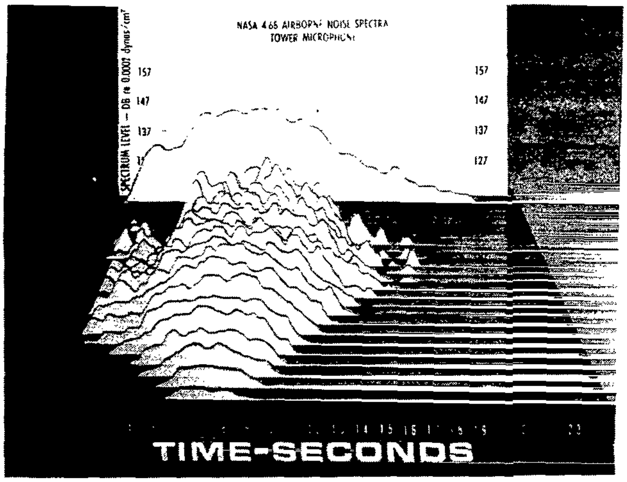

Figure 32—Front view of the three-dimensional plot of NASA 4.68 overall noise level and one-third octave analysis—tower microphone 10.0 kc LPOF.

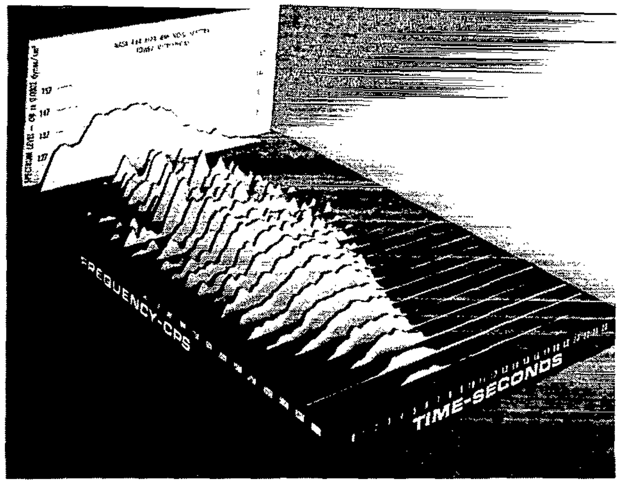

Figure 33—Left oblique view of the three-dimensional plot of NASA 4.68 overall noise level and one-third octave analysis—tower microphone.

BIBLIOGRAPHY

"Aerobee-150A Sounding Rocket Model AJ 60-13," Aerojet-General Corporation: Technical Manual Service Instructions, Publication No. HS-520104, June 1960.

Newell, Homer E., Jr., "Sounding Rockets," New York: McGraw-Hill, 1959, p. 89.

Russell, W. A., Jr., "NASA 4.20 Post Flight Summary," Goddard Space Flight Center.

Russell, W. A., Jr., "NASA 4.68 Post Flight Summary," Goddard Space Flight Center, January 26, 1962.

NASA-Langley, 1964 G-526

2/7/85
C6

"The aeronautical and space activities of the United States shall be conducted so as to contribute . . . to the expansion of human knowledge of phenomena in the atmosphere and space. The Administration shall provide for the widest practicable and appropriate dissemination of information concerning its activities and the results thereof."

—NATIONAL AERONAUTICS AND SPACE ACT OF 1958

NASA SCIENTIFIC AND TECHNICAL PUBLICATIONS

TECHNICAL REPORTS: Scientific and technical information considered important, complete, and a lasting contribution to existing knowledge.

TECHNICAL NOTES: Information less broad in scope but nevertheless of importance as a contribution to existing knowledge.

TECHNICAL MEMORANDUMS: Information receiving limited distribution because of preliminary data, security classification, or other reasons.

CONTRACTOR REPORTS: Technical information generated in connection with a NASA contract or grant and released under NASA auspices.

TECHNICAL TRANSLATIONS: Information published in a foreign language considered to merit NASA distribution in English.

TECHNICAL REPRINTS: Information derived from NASA activities and initially published in the form of journal articles.

SPECIAL PUBLICATIONS: Information derived from or of value to NASA activities but not necessarily reporting the results of individual NASA-programmed scientific efforts. Publications include conference proceedings, monographs, data compilations, handbooks, sourcebooks, and special bibliographies.

Details on the availability of these publications may be obtained from:

SCIENTIFIC AND TECHNICAL INFORMATION DIVISION

NATIONAL AERONAUTICS AND SPACE ADMINISTRATION

Washington, D.C. 20546